



HAL
open science

Search for a Higgs boson produced in the vector boson fusion process in the diphoton channel with the ATLAS experiment

E. Petit

► **To cite this version:**

E. Petit. Search for a Higgs boson produced in the vector boson fusion process in the diphoton channel with the ATLAS experiment. Hadron Collider Physics Symposium (HCP2012), Nov 2012, Kyoto, Japan. pp.18018, 10.1051/epjconf/20134918018 . in2p3-01002149

HAL Id: in2p3-01002149

<https://hal.in2p3.fr/in2p3-01002149>

Submitted on 5 Jun 2014

HAL is a multi-disciplinary open access archive for the deposit and dissemination of scientific research documents, whether they are published or not. The documents may come from teaching and research institutions in France or abroad, or from public or private research centers.

L'archive ouverte pluridisciplinaire **HAL**, est destinée au dépôt et à la diffusion de documents scientifiques de niveau recherche, publiés ou non, émanant des établissements d'enseignement et de recherche français ou étrangers, des laboratoires publics ou privés.

Search for a Higgs boson produced in the vector boson fusion process in the diphoton channel with the ATLAS experiment

Elisabeth Petit^{1,a} on behalf of the ATLAS Collaboration

¹LAPP, CNRS/IN2P3 and University of Savoie, Annecy-le-Vieux, France

Abstract. Details of the production of the new particle discovered by the ATLAS experiment at the LHC in the mass region of $m_H = 126$ GeV in the search for the Standard Model Higgs boson at $\sqrt{s} = 7$ TeV and 8 TeV are presented. The addition of a category enriched in vector boson fusion events in the $H \rightarrow \gamma\gamma$ search allows to increase the sensitivity of the search of a Standard Model Higgs boson. It also allows to separate better between gluon fusion and vector boson production modes, thus giving a first insight to the couplings of this newly discovered boson.

1 Introduction

The ATLAS [1] and CMS [2] collaborations have independently reported observations of a new boson compatible with the SM Higgs boson, using the 2011 and 2012 datasets collected until the end of June 2012 [3, 4]. More detailed measurements of this particle is necessary in order to check the compatibility with the Standard Model predictions, in particular the study of the several production modes. These production modes are, by decreasing order of cross-section production: gluon-gluon fusion (noted as ggF), vector boson fusion (VBF), associated production with a vector boson (VH) and associated production with a $t\bar{t}$ pair ($t\bar{t}H$). The expected cross-sections for those four processes, for a center-of-mass energy of 8 TeV and a Higgs mass of 125 GeV are 44.5 fb, 3.6 fb, 2.5 fb and 0.9 fb respectively, when multiplied by the $H \rightarrow \gamma\gamma$ branching ratio (2.28×10^{-3}).

The addition of a category enriched in VBF events allows to improve the sensitivity of the Higgs boson search as well as giving tools to give a first estimate of the couplings of this new boson to fermions and bosons.

2 Event selection

The dataset used in this study is based on 4.8 fb^{-1} of $\sqrt{s} = 7$ TeV data recorded in 2011 and 5.9 fb^{-1} $\sqrt{s} = 8$ TeV data recorded in the first months of 2012 [5].

At least two photons satisfying tight identification criteria based on the shapes of the EM showers are required. The transverse energies for the leading and sub-leading photons are required to be larger than 40 GeV and 30 GeV, respectively, and both need to be within the fiducial calorimeter region of pseudorapidity $|\eta| < 2.37$ (excluding the transition region between the barrel and the end-cap calorimeters, $1.37 < |\eta| < 1.52$).

^ae-mail: Elisabeth.Petit@cern.ch

\sqrt{s}	ggF	VBF	VH	$t\bar{t}H$	total	data
7 TeV	70.9	5.8	3.7	0.3	80.7	23788
8 TeV	100.3	8.3	5.0	0.5	114.1	35271

Table 1. Number of events in the data and number of expected signal events for $m_H = 125$ GeV [5]

In addition to the identification criteria, both photons are also required to be isolated: the transverse energy sum of positive-energy topological clusters deposited in the calorimeter around each photon in a cone of $\Delta R^1 = 0.4$, and is required to be less than 4 GeV. The resolution of the diphoton mass is dominated by the photon energy resolution.

The number of selected data events and expected signal events for $m_H = 125$ GeV after the full selection is given in table 1.

3 Categorisation

The data is divided into 10 exclusive categories with different signal-to-background ratios and different invariant mass resolution. This increases the sensitivity of the search. The first nine categories are described in [5] and are based on the information of the η and conversion status of the photons, as well as the diphoton transverse momentum orthogonal to the diphoton thrust axis in the transverse plane ($p_{T\perp}$). The use of the categories based on $p_{T\perp}$ already gives a separation between VBF and ggF events, the former having larger $p_{T\perp}$ values. The tenth category is based on jets and described in the following.

¹ $\Delta R = \sqrt{\eta^2 + \varphi^2}$, where φ is the azimuthal angle around the beam line

3.1 Definition of the 2-jet category

The definition of a VBF-enriched category (called "2-jet category") is based in the kinematic properties of the VBF for which two forward jets are produced. Jets are reconstructed from three-dimensional clusters of energy in the electromagnetic and hadronic calorimeters using the anti- k_r [6] algorithm with a distance parameter of $R = 0.4$. Jets candidates are required to have a transverse momentum greater than 25 GeV, expect for the $\sqrt{s} = 8\text{TeV}$ data where the threshold is 30 GeV for $2.5 < |\eta| < 4.5$.

This category collects events containing at least two jets with a pseudorapidity separation $|\Delta\eta|$ larger than 2.8 and an invariant mass greater then 400 GeV. In addition, the azimuthal angle difference $|\Delta\phi|$ between the diphoton and the dijet systems is required to be larger than 2.6. Those variables are presented in figures 1 and 2 for VBF and ggF produced signal as well as background. One can see that those variables are used to distinguish between VBF and ggF as well as between VBF and background.

As those cuts, the fraction of VBF events in this category is of 76.7% and 68.4% for the $\sqrt{s} = 7$ and 8 TeV respectively.

3.2 Signal properties and uncertainties

Figure 3 shows the diphoton invariant mass ($m_{\gamma\gamma}$) distribution in the "2-jet category" for the $\sqrt{s} = 7$ and 8 TeV data events. For the $\sqrt{s} = 8$ TeV processes, the signal-to-background ratio in a window containing 90% of the signal is 0.22, which has to be compared to 0.03 in the inclusive case. This high signal-to-background ratio explains the increase of sensitivity due to this category. The mass resolution (FWHM) in this category is 3.7 GeV, similar to the one in the inclusive case (3.9 GeV).

The introduction of jets to define this category added uncertainties related to them. The main one comes from the perturbative uncertainty on the gluon fusion contribution to this category, and is found to be 25%. The production cross-section of a Higgs boson via gluon fusion associated with two jets is only known at the Next-to-Leading Order, and higher-order logarithmic contributions are presented in this limited region of phase space. This large uncertainty is fortunately compensated by the small contribution of ggF events in the category (22.5% and 30.4% for $\sqrt{s} = 7$ TeV and 8 TeV respectively). The uncertainty due to the modelling of the underlying event is estimated by comparing different underlying event tunes in the simulation. For the 2-jets category, a 30% uncertainty is assigned to the contribution from ggF , VH and $t\bar{t}H$, and a 6% uncertainty is assigned to the contribution from VBF. The experimental uncertainties on the jet energy scale is evaluated by varying the scale corrections within their respective uncertainties. The uncertainty for the different classes of categories and different production processes amount to up to 19% for the "2-jet category".

4 Results

The statistical procedures used to test the background-only hypothesis takes the form of statistical tests of different hy-

pothesized values of a strength parameter μ , defined as the ratio of the signal rate (cross section) being tested to that predicted by the SM. That is, $\mu = 0$ is the background-only hypothesis and $\mu = 1$ is the SM hypothesis. At fixed values of the Higgs boson mass m_H , different values of μ are tested using a statistic based on the profile likelihood ratio. To quantify discovery significance, the p -value of the background-only hypothesis, p_0 , is reported and can be seen in figure 4. Equivalently, this can be expressed using the discovery significance. By using an inclusive study, the expected (observed) significance is 1.9σ (3.5σ), whereas by using the 10 exclusive categories, the expected (observed) significance is 2.4σ (4.7σ). Adding a tenth category improves the expected significance by a few percents.

5 Higgs boson coupling properties

Because of a category sensitive to the VBF, it is possible to study the contributions from the different production modes, in order to assess any tension between the data and the ratios of the production cross-sections in the Standard Model. For each production mode, a signal strength is defined, which is defined by $\mu_i = \sigma_i/\sigma_{i,SM}$. Production modes have been grouped together: μ_{ggF} with $\mu_{t\bar{t}H}$ as they scale with the $t\bar{t}H$ coupling, and μ_{VBF} with μ_{VH} as they scale with the WWH and ZZH couplings in the Standard Model. Constraints in the plane of $\mu_{ggF+t\bar{t}H} \times B/B_{SM}$ (where B is the branching ratio for $H \rightarrow \gamma\gamma$) and $\mu_{VBF+VH} \times B/B_{SM}$ can be seen in figure 5, for $m_H = 126$ GeV. The data are compatible with the Standard Model expectation at the 1.5σ level.

The coupling properties of the boson can be further studied by combining results from several decay channels: $H \rightarrow \gamma\gamma$, $H \rightarrow ZZ$, $H \rightarrow WW$, $H \rightarrow \tau\tau$, and $H \rightarrow b\bar{b}$ [7]. The leading order (LO) motivated scale factors κ_i are defined in such a way that the cross sections σ_{ii} and the partial decay widths Γ_{ii} associated with the SM particle i scale with the factor κ_i^2 when compared to the corresponding SM prediction.

For example, among the production modes, $\kappa_g^2 = \frac{\sigma_{ggF}}{\sigma_{ggF}^{SM}}$, $\kappa_{WH}^2 = \frac{\sigma_{WH}}{\sigma_{WH}^{SM}}$, etc, and among the decay modes, $\kappa_\gamma^2 = \frac{\Gamma_{\gamma\gamma}}{\Gamma_{\gamma\gamma}^{SM}}$, $\kappa_W^2 = \frac{\Gamma_{WW^{(*)}}}{\Gamma_{WW^{(*)}}^{SM}}$, etc.

The couplings to fermions and vector bosons are studied by assuming scale factors κ_F for the couplings to all fermions and κ_V for the couplings to all vector bosons:

$$\begin{aligned} \kappa_F &= \kappa_t = \kappa_b = \kappa_\tau \\ \kappa_V &= \kappa_W = \kappa_Z \end{aligned} \quad (1)$$

By assuming that the total width of the Higgs boson is given by the sum of the known SM Higgs boson decay modes, the constraints in the κ_F and κ_V plane are given in figure 6. The 68% CL intervals when profiling over all other parameters are: $\kappa_F \in [-1.0, -0.7] \cup [0.7, 1.3]$ and $\kappa_V \in [0.9, 1.0] \cup [1.1, 1.3]$. The compatibility of the SM hypothesis with the best fit point is 21%.

References

[1] ATLAS Collaboration, JINST 3 S08003 (2008)
 [2] CMS Collaboration, JINST 3 S08004 (2008)
 [3] CMS Collaboration, Phys.Lett.B716, 30-61 (2012), arXiv:1207.7235

[4] ATLAS Collaboration, Phys.Lett.B716, 1-29 (2012), arXiv:1207.7214
 [5] ATLAS Collaboration, ATLAS-CONF-2012-091 (2012), http://cds.cern.ch/record/1460410
 [6] M. Cacciari, G.P. Salam, G. Soyez, JHEP 0804 (2008)
 [7] ATLAS Collaboration, ATLAS-CONF-2012-127 (2012), http://cds.cern.ch/record/1476765

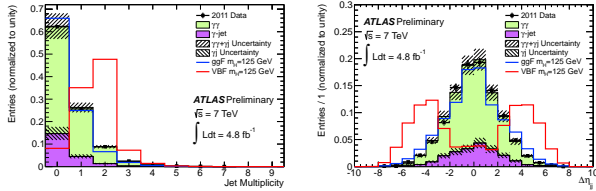


Figure 1. Jet multiplicity and η separation of the leading and subleading jets for $\sqrt{s} = 7$ TeV compared to simulation. The diphoton component is simulated with SHERPA, while the γ -jet component is simulated with ALPGEN, and the small jet-jet and Drell-Yan components are neglected. The distributions are normalized to unit area [5].

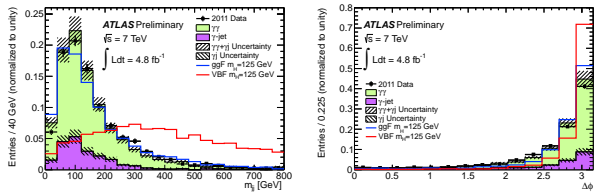


Figure 2. Dijet invariant mass and φ separation between the diphoton and the dijet system for $\sqrt{s} = 7$ TeV compared to simulation. The diphoton component is simulated with SHERPA, while the γ -jet component is simulated with ALPGEN, and the small jet-jet and Drell-Yan components are neglected. The distributions are normalized to unit area [5].

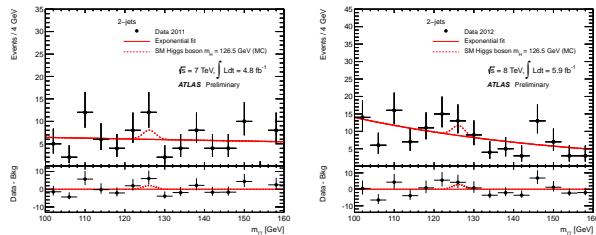


Figure 3. Background-only fit to the diphoton invariant mass spectra for the category 2-jets, for $\sqrt{s} = 7/8$ TeV. The bottom inset displays the residual of the data with respect to the background fit. The Higgs boson expectation for a mass hypothesis of 126.5 GeV corresponding to the SM cross section is also shown [5].

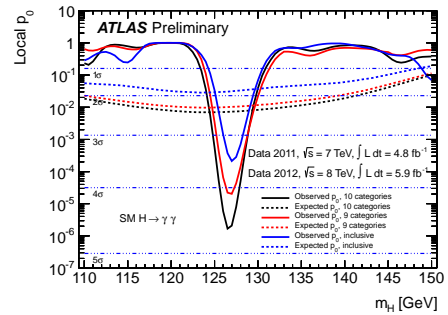


Figure 4. Expected and observed local p_0 for the analysis using 10 categories, compared to an analysis using only 9 categories (no 2-jets category) and a fully inclusive analysis for the combined $\sqrt{s} = 7$ TeV and $\sqrt{s} = 8$ TeV data [5].

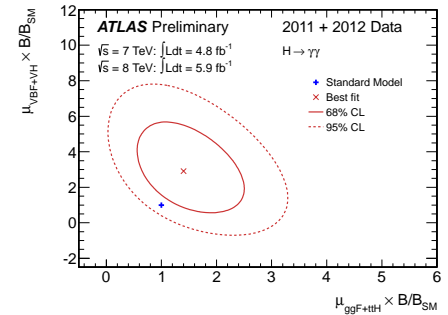


Figure 5. Measurements of the signal strength parameter μ for $m_H = 126$ GeV for the individual channels and their combination. [7].

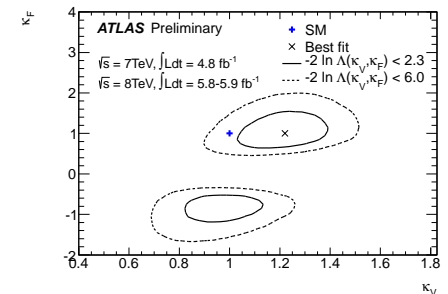


Figure 6. Fits for 2-parameter benchmark models probing different coupling strength scale factors for fermions and vector bosons; in this case the correlation of the coupling scale factors κ_F and κ_V , assuming no non-SM contribution to the total width [7].